We P05 02

Potential Applications of Time-lapse Marine CSEM to Reservoir Monitoring

O. Salako* (Heriot-Watt University), C. MacBeth (Heriot-Watt University), L. MacGregor (RSI) & E. Mackay (Heriot-Watt University)

SUMMARY

Three different oil field production settings are identified where time-lapse marine CSEM could find reservoir monitoring application. One of these settings, low salinity water injection, is given particular attention in this work. We generate time-lapse CSEM amplitude data from a 3D fluid flow simulation model by converting the dynamic changes to resistivity changes, and then employing 1D–dipole forward modelling for an in-line acquisition geometry. We utilise a rock physics model that accounts for heterogeneity, and takes into consideration the time variations in the salinity and temperature profile to calculate the vertical resistivity for each simulator cell. The modelling uses as a guide a full field model for a North sea turbidite reservoir into which low salinity water is injected. Measuring the three amplitude components of the CSEM survey, it is concluded that time lapse CSEM has the potential to be used qualitatively to monitor the evolution of low salinity water injection.

Introduction

Over the years, several studies have been performed to examine the applications of marine Controlled Source ElectroMagnetic (CSEM) to reservoir monitoring. For example: Lien & Mannseth (2008) used an integral equation approach to model the 3D time-lapse effect of a lateral water flooding process; Orange et al. (2009) used a 2D finite element approach to study lateral and basal waterflooding. These studies demonstrated a measurable time-lapse CSEM signal attributable to production and injection activities, however the assumption of sharp waterfront is not realistic in practice. Thus, Shahin et al. (2010) and Liang et al. (2011) utilised a fluid-flow reservoir simulator, to generate a realistic water front in their studies, in which they further confirmed the potential of using marine CSEM to monitor water flooding. Recently, Salako et al. (2012) considered a practical simulator to CSEM tool driven by the 1D dipole method of Key (2009), which also accounted for variable net-to-gross in the reservoir. This permitted a direct comparison with simulator to seismic methods, (described by Amini et al., 2012), regarding the relative sensitivities of water saturation detection, particularly in the presence of variable reservoir thickness, net-to-gross and porosity.

In this context, further rock physics work has identified three specific oilfield production/recovery settings where time-lapse CSEM could be suitable for reservoir monitoring: (1) low salinity (500ppm) water injection into a reservoir containing saline formation water (such as in the northwest of the UK, with a salinity of 18,000ppm); (2) fluid contact movement in the giant carbonate and sandstone reservoirs of Saudi Arabia, where injected water with 10,000ppm average salinity obtained from a overlying massive sandstone aquifer assists production of hydrocarbons containing formation water of very high salinities ranging from 180,000 to 220,000ppm; (3) seawater of 15°C temperature and 30,000ppm salinity injected into a North sea reservoir with formation water of temperature of 60°C and salinity of 18,000ppm. For the purpose of this present work, we consider the first application as the focus for an in-depth modelling study using our simulator to CSEM methodology.

Low salinity water flooding is an emerging technology for enhanced oil recovery, in which the injected water also chemically reacts with the formation to increase the water wetness of rock. Although the precise action of low salinity water is still debatable, it is understood that increased water wetness does enhance mobility of the bound oil. The increased water wetness results in higher relative permeability for oil and lower relative permeability for water. Indeed, this is proven to enhance the oil recovery over an equal volume of injected water. Another benefit of such waterflooding is the reduction in chemical scaling and corrosion of the equipment used in the oil field (for example: Tang & Morrow, 1997; Jerauld et al., 2008). In a waterflood, knowledge of how the low salinity water distributes amongst the other fluids is desirable as this determines its efficiency. This is important, as low salinity water may not flow through the reservoir in the same way as normal higher salinity water. To address this objective, here we model the CSEM response to determine the likely potential of monitoring such a waterflood, relative to the use of seawater injection.

Rock physics modelling

Using Archie's equation (Archie, 1942), and assuming a series arrangement of sand and shale resistivities scaled with the spatial distribution of net-to-gross, Salako et al. (2012) propose a relation for the resistivity R_t of the fluid-saturated reservoir rock

$$R_t = NTG\frac{aR_w}{\Phi^m S_w^n} + (1 - NTG)R_{sh} \qquad (1)$$

where R_w, NTG, Φ, S_w and R_{sh} are the water resistivity, net-to-gross, effective (sand) porosity, water saturation and the shale resistivity respectively. Archie constants of a =1; n = 2 are chosen, while the cementation factor m is calculated from well logs. Ross (2000) expressed water resistivity as a function of temperature and salinity based on laboratory measurement

$$R_w = \left(\frac{400{,}000}{Temp \times Sal}\right)^{0.88} \qquad (2)$$

where, *Temp* and *Sal* are temperature and salinity respectively. Equation (2) agrees with the value of R_w calculated by the log interpretation chart Gen-6 (Schlumberger online resource) which relates resistivity of water with temperature and salinity. This permits the resistivity to be calculated for any salinity and temperature combination.

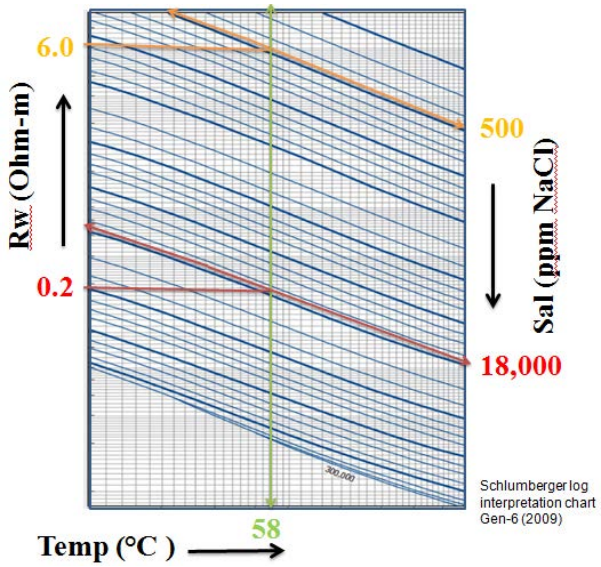

Figure 1 *The range of resistivity values for mixed water as a function of salinity and temperature (Schlumberger online resource). Here we show the example of low salinity (500ppm) water injection into a reservoir with saline (18,000ppm) formation water at fixed temperature (58°C). The resultant resistivity scaling is 30 times. This illustrates the motivation for this work, and demonstrates the differences anticipated from our production/recovery scenarios.*

Figure 1 illustrates the first case of the oilfield production/recovery settings stated above, low salinity water injection. Here, native formation water with salinity of 18,000ppm and injected low salinity water of 500ppm produce the resistivities of 0.2Ωm and 6.0Ωm respectively. Thus we have a factor of 30 in resistivity, which provides good motivation to continue the modelling work. We assume the process of desalinating seawater may raise the temperature, and slightly lower the resistivity. However, as the effect of temperature on the injected water is mainly concentrated around the injection well, and the injected water rapidly assumes the formation temperature as it progresses outwards towards the producer, this is therefore not considered to be a significant effect.

This figure can also be used to examine the CSEM applicability in the two other settings we have identified. For the second case, where aquifer water with 10,000ppm average salinity is injected to assist hydrocarbon production from reservoirs containing formation water of very high salinities ranging from 180,000 to 220,000ppm (average of 200,000ppm), the objective is to monitor the fluid saturations at oil-water contact and behind the water front, where formation water has been pushed into a defined connate-water bank by the injected water (Rafle & Youngblood, 1987). Using an average reservoir temperature of 65°C (Nasr-El-Din et al., 2002), the resistivities of the formation and injected waters are 0.034Ωm and 0.3Ωm respectively; this is a factor of 9 in resistivity. In the third case, seawater of 15°C temperature and 30,000ppm salinity is injected into a North sea reservoir with formation water of temperature of 60°C and salinity of 18,000ppm, producing resistivities of 0.27Ωm and 0.2Ωm respectively. This a common occurrence, and is used here as a reference point to examine the impact of seawater injection on time-lapse CSEM monitoring.

Simulator to CSEM modelling

For the purposes of this current study we focus on a field simulation model from a heterogeneous deep-water turbidite system on the UK continental shelf, containing sand channels and sheets interbedded with shale layers. Initially, we carry out a brine tracking reservoir simulation based on Jerauld et al. (2008). Two sets of brine tracking fluid flow simulations are performed, the first with

injected seawater of salinity 18,000ppm (identical to the formation water). Next low salinity 500ppm water is injected and the reservoir properties adapted to become 10% more water-wet. This is achieved by making adjustments to the relative permeability table for the simulator. The low salinity water injection produced about 8MM (STB) of extra oil over the conventional high salinity seawater injection at the end of a ten year period. Figures 2(a) and (b) show maps of the changes in saturation and salinity respectively. After the simulations, the resistivity value for each simulation cell is calculated from equations (1) and (2), and these are then used to model the CSEM electric or magnetic field signals. For modelling purposes, the reservoir is buried between 1.8 and 2.0km below the seafloor and at 400m water depth. The seawater and seabed resistivities are set to 0.3Ωm and 1Ωm respectively. A dipole transmitter at 1Hz frequency is towed 25m above, and parallel to the seafloor receiver, with a transmitter–receiver spacing of 500m and from zero to 15km total offset. We model four CSEM suveys, the baseline (before production) and three monitors (after three, six and ten years of low salinity injection) according to Salako et al. (2012). All of the surveys generate a measurable signal above the noise floor expected for this water depth and background structure. Three percentage time-lapse amplitude maps for (2001 – 1998), (2004 – 1998) and (2008 – 1998) were obtained by calculating absolute differences in amplitudes of the electric and magnetic responses between each of the monitor surveys and the baseline survey, normalised with the baseline amplitude.

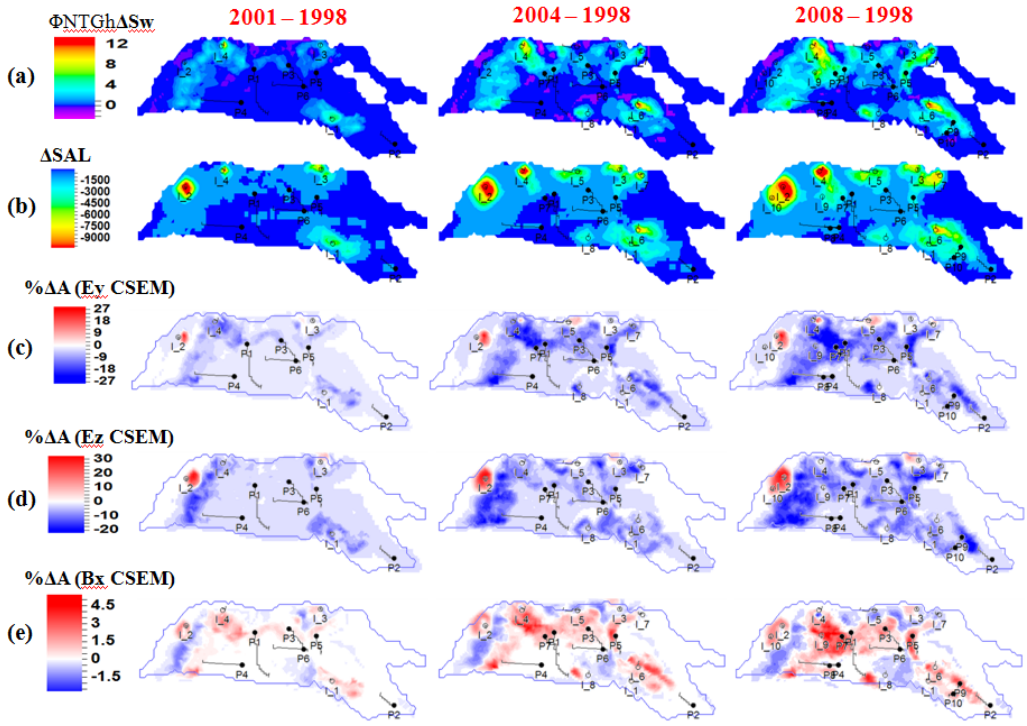

Figure 2 *Maps of changes in: (a) Water saturation scaled with static reservoir parameters, (b) Salinity, (c) Inline electric field component, (d) Vertical electric field component and (e) Cross-line magnetic field component, generated for three time-lapse periods (2001 – 1998), (2004 – 1998) and (2008 – 1998).*

Qualitative interpretation of results

Figures 2(c), (d) and (e) show the resultant percentage timelapse CSEM amplitudes for the horizontal electric (%ΔEy), vertical electric (%ΔEz) and crossline magnetic (%ΔBx). For %ΔEy and %ΔEz, a very high negative timelapse anomaly (deep blue colour) indicates areas of the reservoir away from the injectors, toward producers (e.g. away from injectors I2 and I4 towards producers P3 and P4), where the formation water (with a low resistivity of 0.2Ωm) has displaced oil (with a higher resistivity of 60Ωm). There is a reduced anomaly (light blue colour) within the areas of high initial oil saturation (e.g. right hand corner of the reservoir), where a large portion of the injected low salinity water (with a high resistivity of 6Ωm) mixed with some portion of low resistivity formation water has displaced higher resistivity oil (e.g. around injectors I1, I6, I8 and producers P2, P6, P10). Close to the injectors, where injected low salinity water displaces saline formation water (connate-water banking), we

observe a positive timelapse response (red colour). A similar interpretation follows for %ΔBx, however the polarity of the changes is reversed compared to the electric field results. In this 1D analysis, the magnitude of the mapped amplitudes varies directly with the volumetric proportion of replacement. Note that the time-lapse amplitude changes in CSEM show significant differences between the various production scenarios, whereas the response to injected seawater of equal salinity (18,000ppm) as the formation water is smaller. For example, the %ΔEy amplitude for the seawater injection case ranges between 0% and -32% (Salako et al, 2012); while for the low salinity (500ppm) water injection case, %ΔEy ranges between 27% and -27% for the same timelapse period.

Conclusion

We have shown that time-lapse CSEM amplitudes show a strong sensitivity to changes in both saturation and salinity induced by low salinity water injection, and therefore suggests that CSEM is a potentially useful tool for monitoring the evolution of low salinity water injection.

Acknowledgements

We thank sponsors of the Edinburgh Time Lapse Project, Phase IV and V (BG, BP, CGGVeritas, Chevron, ConocoPhillips, ENI, ExxonMobil, Hess, Ikon Science, Landmark, Maersk, Marathon, Nexen, Norsar, Petrobras, RSI, Shell, Statoil, Suncor and Total) for supporting this research. We thank Schlumberger-Geoquest for the use of Petrel and Eclipse software. O. Salako acknowledges financial sponsorship of his PhD by the Petroleum Technology Development Fund, Nigeria. He is on leave of absence from the Department of Geology, Osun State University, Nigeria.

References

Amini, H., Alvarez, E., MacBeth, C., & Shams, A. [2012] Finding a petro-elastic model suitable for sim2seis calculation. Copenhagen: 74th EAGE Conference.

Archie, G. E. [1942] The electrical resistivity log as an aid in determining some reservoir characteristics. *Petroleum Transactions of the AIME,* ***146***, 54–62.

Jerauld, G. R., Lin, C. Y., Webb, K. J., & Seccombe, J. C. [2006] Modeling Low-Salinity Waterflooding. San Antonio: Society of Petroleum Engineers.

Key, K. [2009] 1D inversion of multicomponent, multifrequency marine CSEM data: Methodology and synthetic studies for resolving thin resistive layers. *Geophysics,* ***74***(2), F9-F20.

Liang, A., Abubakar, A., & Habashy, T. M. [2011] Feasibility study of marine CSEM for reservoir monitoring using joint 3D EM modeling and fluid flow simulator. Vienna: 73rd EAGE Conference.

Lien, M., & Mannseth, T. [2008] Sensitivity study of marine CSEM data for reservoir production monitoring. *Geophysics,* ***73***(4), F151-F163.

Nasr-El-Din, H. A., Lynn, J. D., Hashem, M. K., & Bitar, G. [2002] Field Application of a Novel Emulsified Scale Inhibitor System to Mitigate Calcium Carbonate Scale in a Low Temperature, Low Pressure Sandstone Reservoir in Saudi Arabia. San Antonio, Texas: Society of Petroleum Engineers.

Orange, A., Key, K., & Constable, S. [2009] The feasibility of reservoir monitoring using time-lapse marine CSEM. *Geophysics,* ***74***(2), F21-F29.

Rafle, M. Y., & Youngblood, W. E. [1987] Advances in Quantitative Reservoir Description and Monitoring in Saudi Arabia. *12th World Petroleum Congress.* Houston, USA: World Petroleum Congress.

Ross, E. R. [2000] *Crain Petrophysical Online Handbook*. Retrieved November 30, 2011, from http://www.spec2000.net/00-resume.htm

Salako, O., MacBeth, C., & MacGregor, L. [2012] Towards joint interpretation of CSEM Surveys with 4D Seismic for Reservoir Monitoring. Copenhagen: 74th EAGE Conference.

Tang, G. Q., & Morrow, N. R. [1997] Salinity, Temperature, Oil Composition, and Oil Recovery by Waterflooding. *SPE Reservoir Engineering,* ***12***(4), 269-276.